Computational and Experimental Determination of the α−Helix Unfolding Reaction Coordinate †

ARTICLE *in* BIOCHEMISTRY · MARCH 2008

Impact Factor: 3.02 · DOI: 10.1021/bi702112v · Source: PubMed

4 AUTHORS, INCLUDING:

Sanford A Asher
University of Pittsburgh
311 PUBLICATIONS **13,067** CITATIONS
SEE PROFILE

Jeffry D Madura
Duquesne University
160 PUBLICATIONS **19,169** CITATIONS
SEE PROFILE

Computational and Experimental Determination of the α-Helix Unfolding Reaction Coordinate†

Eliana K. Asciutto,*,‡ Aleksandr V. Mikhonin,§ Sanford A. Asher,§ and Jeffry D. Madura‡

Department of Chemistry and Biochemistry, Center for Computational, Sciences, Duquesne University, Pittsburgh, Pennsylvania 15282, and Department of Chemistry, University of Pittsburgh, Pittsburgh, Pennsylvania 15260

Received October 19, 2007; Revised Manuscript Received December 13, 2007

ABSTRACT: We demonstrate a calculated α-helix peptide folding energy landscape which accurately simulates the first experimentally measured α-helix melting energy landscape. We examine a 21-amino acid, mainly polyalanine peptide and calculate the free energy along the Ψ Ramachandran angle secondary folding coordinate. The experimental free energy landscape was determined using UV resonance Raman spectroscopy. The relative free energy values are very close as are the equilibrium peptide conformations. We find 2.3 kcal/mol activation barriers between the α-helix-like and PPII-like basins. We also find that the α-helix-like conformations are quite defective and the α-helix-like structure dynamically samples 3_{10}-helix and π-bulges.

A detailed understanding of the mechanism(s) of protein folding requires elucidation of the reaction coordinate for the process (*1*−*4*). The multidimensionality of this process suggests that, at present, it is almost a hopeless task to develop insight into the mechanism. However, the previous successes of the scientific reductionist approach to developing insight into complex problems offers encouragement to the community of scientists studying protein folding. Probably the most important reaction coordinate for protein folding directs the formation of secondary structure. The obvious coordinates for this structural evolution are the Ramachandran ψ and φ angles. Because the most important secondary structure motifs (folded and unfolded) have widely differing ψ angles but similar φ angles it is probably most important to monitor the ψ angle coordinate.

Recently, we developed a spectroscopic method to determine the value of the peptide bond ψ angle (*5*−*8*). This novel method directly correlates the frequency of the $AmIII_3$ vibration enhanced in the resonance Raman spectra to the ψ angle value of a particular peptide bond. The ψ angle distribution can then be related to the free energy. The $AmIII_3$ frequencies of a mainly ala, 21-residue peptide known as AP were monitored by using UV Raman excitation at ∼200 nm exciting within the amide $\pi \rightarrow \pi^*$ electronic transitions. It was found that the energy landscape along the ψ angle coordinate has modest barriers between the α-helix-like conformations and the melted PPII-like and turn conformations. Indeed, the α-helix-like basin is broad and contains significant populations of defects such as 3_{10} and π-bulges. These Raman studies were the first to experimentally determine folding energy landscapes and activation barriers; it is essential to test these experimental results to see if they can function as benchmarks for theoretical calculations that model folding. Thus, in this paper we examine a molecular dynamics simulation of α-helical melting for AP. AP is mainly α-helical at 273 K and melts fully to a PPII-like conformation as the temperature increases to 323 K.

AP is an ideal model for our testing purpose due to the extensive experimental (*9*−*13*) and computational (*14*−*17*) work that has been done. Garcia et al. performed a replica exchange molecular dynamics (REMD) simulation ∼1.7 μs long comparing AP to a polyalanine (A21) helix. They concluded that the arginine side chains produce a shielding effect that stabilizes α-helical conformations. The shielding effect is proposed to be due the interaction between the charged side chain and the backbone carbonyl oxygens.

They also pointed out that the helix content for polyalanine peptides depends on the force field. Therefore, in order to obtain better agreement with the experimental data, they introduced a modification to the AMBER-94 force field (*18*) by setting the torsion potential for ϕ and ψ to zero (*14*). This modification reproduced experimental propagation and nucleation parameters more accurately.

Zhang et al. performed an all-atom simulation using a modified AMBER-94 force field (*19*) with the generalized Born solvent model (GB). The modified AMBER-94 force field was determined by fitting the electrostatic potentials of dipeptides calculated using quantum mechanical methods. Using this modified AMBER-94 force field Zhang et al. reported that AP unfolding is a two-state process where the 300 K minimum energy configuration is a 'helix-turn-helix (HTH)', while the minimum energy configuration at 273 K is a pure helix.

† J.D.M. thanks the Pittsburgh Supercomputing Center (SEE050005P) and the Supercomputer Allocations Board (MCB060059P) for providing generous computing resources. Some of the computations were performed on the HPQ Alpha-SC system Ben as well as the Cray XT1 (BigBen) at the Pittsburgh Supercomputing Center. The Center for Computational Sciences is partially supported by the National Science Foundation CHE-0321147. The experimental work was supported by NIH grant GM8RO1EB0020053 (S.A.A.).

* Author to whom correspondence should be addressed. Telephone: 412-396-6341. Fax: 412-396-5683. E-mail: ekasciut@gmail.com.

‡ Duquesne University.

§ University of Pittsburgh.

10.1021/bi702112v CCC: $40.75
Published on Web 01/12/2008

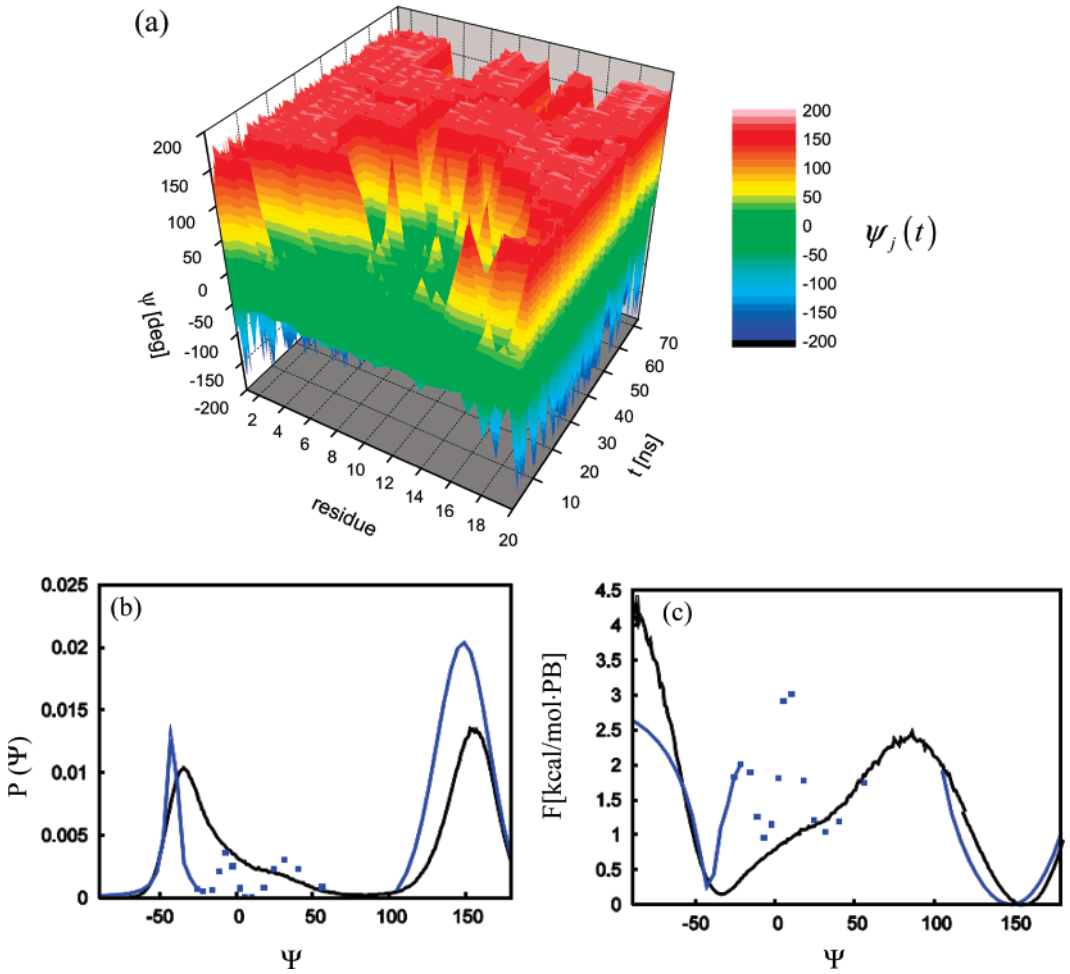

FIGURE 1: (a) Temporal evolution of the set $\Psi = \{\psi_j\}$: The value of each dihedral angle ψ_j as a function of the residue j and the time t in ns. During the first 20 ns the angles are in the α-helical region (green) and later evolving to a PPII region (red). (b) Ψ angle distribution from a 70 ns molecular dynamics simulation at 300 K in explicit water. Experimental UV Raman distribution is also shown in blue. (c) Helmholtz free energy landscape in kcal/mol·peptide bond from the molecular dynamics simulation for the unfolding reaction associated with the reaction coordinate. The experimentally calculated Gibbs free energy landscape in kcal/ mol·peptide bond is shown in blue.

In a comparison of the GB model versus explicit solvent, Nymeyer and Garcia (*20*) showed that GB favors configurations such as the HTH, suggesting that the greater stability of HTH is an artifact of the GB model. Sorin et al. performed an all atom study of AP in an explicit solvent. Using a global distributed computer network (Folding@Home) they extensively sampled AP configurations. In these calculations they used a modified AMBER-99 force field, changing the backbone torsional potentials to achieve better agreement with experimental parameters characterizing the unfolding reactions.

They reported that the AP unfolding landscape is a pseudo two-state process with two broad basins which include a diverse population of conformations which are separated by small barriers. Although the Sorin et al. as well as the Garcia et al. force fields improve the modeling of alanine-based peptides, they still fail to reproduce some experimentally observed features and parameters as the Lifson−Roig (*8*, *16*). In a novel paper, Chodera et al. (*17*) reported the development of an algorithm to calculate long-lived, kinetically metastable states. Using Sorin et al.'s molecular dynamics simulation data of AP, Chodera et al. identified 20 different conformational states for AP. The different conformational states identified included minima and metastable states such as extended coil, pure helix, helix-coil bent in half, and helical states bent in circles. These last two metastable states are similar to the HTH and GH conformers reported by Zhang et al.

In the work here we employed a very recent modification of the AMBER-99 force field (ffSB99) (*21*), which have improved ϕ and ψ potential parameters to achieve a better balance of the dihedral angle distributions for glycine and alanine. Our objective is to more realistically model the α-helix unfolding process.

RESULTS AND DISCUSSION

In our molecular dynamics simulation the initial state of the peptide was completely α-helix and immersed in explicit TIP3P water (*22*). We monitored the time-dependent set of ψ_j dihedral angles:

$$\Psi(t) = \{\psi_1(t),\psi_2(t),...,\psi_j(t),...,\psi_{res-1}(t)\} \qquad (1)$$

where ψ_j is the dihedral angle between residue j and $j + 1$ and res is the total number of residues. We ran a 70 ns molecular dynamics simulation at 300 K with AMBER9 (*23*) using the ffSB99 force field. All the details of the simulations are given in the Supporting Information.

The time scale of our simulation should be long enough to reach equilibrium, since the Sorin et al. study previously

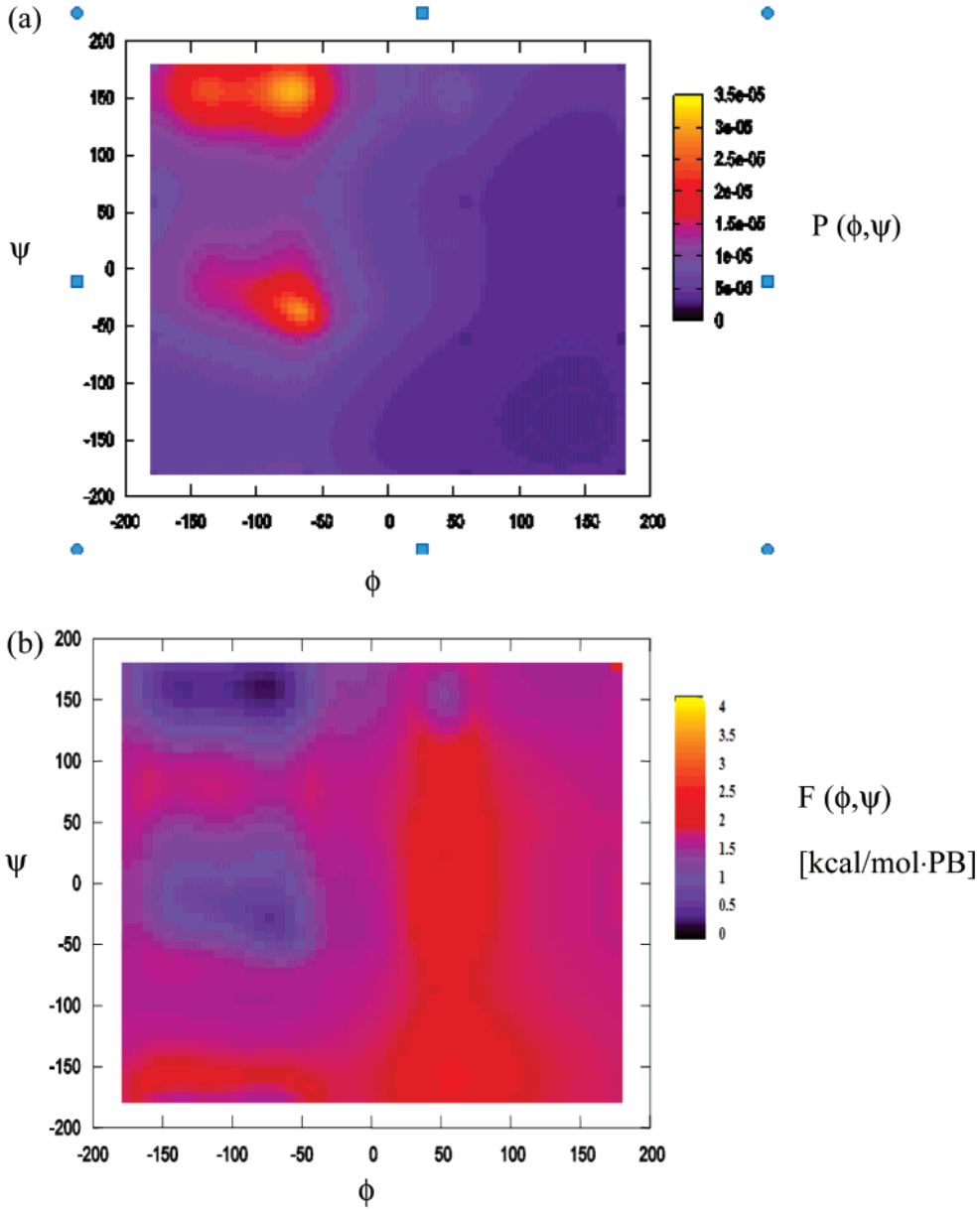

FIGURE 2: (a) Normalized probability density of the dihedral pairs (ϕ,ψ) during the unfolding process. The two yellow regions show the two more populated states in the helical and extended regions. (b) Helmholtz free energy profile in kcal/mol·PB as a function of the pairs (ϕ;ψ) obtained from the probability distribution.

demonstrated that the helical conformational equilibrium is reached within 25 ns in their molecular dynamics simulation using REMD with AMBER force fields (*16*). However, this contrasts sharply with our experimentally determined relaxation rates for AP α-helix melting which span the 200 ns to 2 μs time regime (*13*, *27*, *28*). We are currently examining the origin of this important large difference between simulation and experimentally determined relaxation timescales.

By trajectory inspection, we found that α-helical AP starts unfolding within ~ 20 ns. The dynamics of the unfolding in terms of $\psi_j(t)$ is illustrated in Figure 1(a). During the first 20 ns all $\psi_j(t)$ values remain in the α-helix region, with values ~−40° (green region). Then, starting from the terminal residues, the peptide begins to unfold with ψ_j dihedral angles flipping to ~150° (red region), a value associated with the PPII configuration. The backbone ψ dihedral angles involving the arginine evolve more slowly, remaining α-helical for longer times. These arginine dihedral angles also resample α-helical values during the simulation (Figure 1(a)). Each ψ_j clearly samples two well defined conformational regions, the initial α-helix-like folded region (green) and an unfolded region (red). We also observe intermediate ψ_j values between 0° to 50° (yellow).

We utilized the temporal evolution data to calculate the Ψ angle distribution (Figure 1(b)). The folded α-helix-like state is represented by the peak centered at Ψ = −36°, while the unfolded state gives rise to a second peak centered at Ψ = 153°. The sampled α-helix-like region has a broader Ψ angle basin than does the PPII-like region, with a significant occupation of Ψ dihedral angle values in the 0° to 50° range. These states involve conformations where two short helices occur which are separated by a turn region and confomations involving helices bent in circles as reported by Zhang et al. and Sorin et al. (*15*, *16*).

The UV Raman determined Ψ distribution is also shown (blue in Figure 1b) which also finds two peaks, an α-helix-

like peak at $\Psi = -42° \pm 5°$ and an unfolded PPII-like state at $\Psi = 145° \pm 5°$. The UV Raman results find discrete values and do not find a continuous distribution of Ψ angles between $\Psi = -30°$ to $\Psi = 50°$, shown by the points in Figure 1. The UV Raman studies also estimated population distributions for particular turn configurations at discrete Ψ values as shown by the blue points in Figure 1.

We also calculated the ϕ_j dihedral angle distribution and found it was sharply peaked at $\Phi = -68°$ (Figure 2(a)), a value in the range assigned to PPII conformations (*24*). We find other populated Φ angles at $\sim -120°$, which probably derive from β strands. We clearly find that a PPII-like conformation dominates the distribution, as found in our Raman results (*7*, *8*). Furthermore, the calculations indicate that the transition state is spanned by peptide bond Ψ angles ranging from 50° to 100°, values normally associated with Type II turns.

From the distribution obtained for Ψ, we calculate a free energy barrier between the folded and unfolded states of 2.3 kcal/mol (Figure 1(c)) which compares very favorably with the UV Raman estimated barrier of between 2.2 and 3.4 kcal/mol.

Our estimated helix-PPII barrier is quantitatively similar to the helix-coil barriers estimated by Young et al. (*25*) for small peptides $(Ala)_n$. It is important to note that Young et al. observed that the helicity depends on the number of residues and that fewer extended structures occur as the number of residues increase. Additionally Tobias et al. (*26*) reported that more turns and extended structures and less helical structures occur for $(Ala)_n$ with $n = 3$. It is known that classical force fields overemphasize the stability of the various secondary structures (*16*). The agreement between our simulation and our UV Raman results clearly indicates that the force field used in this simulation correctly models the equilibrium distribution that exists.

Statistical Interpretation of Ψ. *Median vs Mean.* The reaction coordinate should completely bridge and differentiate all folded and unfolded states. The mean of $\{\psi_j\}$ will be significantly affected when there are a few ψ_j values far from the rest. Figure 1(a) shows that unfolding begins at the terminal residues and propagates inward. Thus the mean $\langle\Psi\rangle$ value would be greatly impacted by terminal residues with ψ_j values not involving folded configurations even if the overall structure were essentially fully α-helical. We utilize the median Ψ value as the statistical quantity that best describes the set Ψ, as opposed to the mean, because the median better monitors the overall conformation of the peptide and is less affected by the terminal residues.

CONCLUSIONS

Our work here is the first to our knowledge to compare simulation derived peptide folding energy landscapes to that determined experimentally. We carried out a molecular dynamics simulation of a mainly polyalanine peptide unfolding reaction and compared the conformational equilibrium and the energy landscape to that determined using UV resonance Raman spectroscopy. The calculated reaction coordinate properly identifies the folded and unfolded conformations. Our calculated free energy barrier between the folded and unfolded states is estimated to be ∼2.3 kcal/mol and is in excellent agreement with the experimental results.

The agreement with experiments validates the use of this force field for modeling α-helix melting in alanine peptides in solution. Both the UV Raman experimental results and the molecular dynamics simulation demonstrates that the AP unfolding process is a pseudo two-state process with a broad basin of folded states containing α-helix-like and helix-turn-helix conformations and a nonrandom unfolded state containing mainly polyproline II conformations.

Finally, we are continuing to use this force field to investigate the mechanism of peptide folding/unfolding. Our studies, for example, correctly find that PPII structures dominate the unfolded state, whereas previously published studies find other structures such as coil, extended, and some also PPII on AP folding/unfolding (*14*−*16*). The major difference between the reported studies and ours is in the number and types of unfolded conformations (e.g., coil, extended, PPII). This discrepancy is due to the different force fields used.

SUPPORTING INFORMATION AVAILABLE

Details of the simulation. This material is available free of charge via the Internet at http://pubs.acs.org.

REFERENCES

1. Portman, J. J., Takada, S., and Wolynes, P. G. (2003) Microscopic theory of protein folding rates. II. Local reaction coordinates and chain dynamics, *J. Chem. Phys. 114*, 5082.
2. Schonbrun, J., and Dill, K. (2002) Fast protein folding kinetics, *Proc. Natl. Acad. Sci. U.S.A. 100*, 12678.
3. Socci, N. D., Onuchic, J. N., and Wolynes, P. G. (1996) Diffusive dynamics of the reaction coordinate for protein folding funnels, *J. Chem. Phys. 104*, 5860.
4. Eaton, W. A. (1999) Searching for "downhill scenarios" in protein folding, *Proc. Natl. Acad. Sci. U.S.A. 96*, 5897.
5. Asher, S. A., Ianoul, A., Mix, G., Boyden, M. N., and Karnoup, A. (2001) Dihedral Ψ angle dependence of the Amide III vibration: A uniquely sensitive UV Resonance Raman secondary structural probe, *J. Am. Chem. Soc. 123*, 11775.
6. Mikhonin, A. V., Bykov, S. V., Myshakina, N. S., and Asher, S. A. (2006) Peptide secondary structure folding reaction coordinate: Correlation between UV Raman Amide III frequency, Ψ Ramachandran angle, and hydrogen bonding, *J. Phys. Chem. B 110*, 1928.
7. Asher, S. A., Mikhonin, A. V., and Bykov, S. (2004) UV Raman demonstrates that α-helical polyalanine peptides melt to polyproline II conformations, *J. Am. Chem. Soc. 126*, 8433.
8. Mikhonin, A. V., and Asher, S. A. (2006) Direct UV Raman monitoring of 3_{10}-helix and π-bulge premelting during α-helix unfolding, *J. Am. Chem. Soc. 128*, 13789.
9. Lockhart, D. J., and Kim, P. S. (1992) Internal Stark effect measurement of the electric field at the amino terminus of an alpha helix, *Science 257*, 947.
10. Lockhart, D. J., and Kim, P. S. (1993) Electrostatic screening of charge and dipole interactions with the helix backbone, *Science 260*, 198.
11. Williams, S. et al. (1996) Fast events in protein folding: Helix melting and formation in a small peptide, *Biochemistry 35*, 691.
12. Thompson, P. A., Eaton, W. A., and Hofrichter, J. (1997) Laser temperature jump study of the helix reversible arrow coil kinetics of an alanine peptide interpreted with a 'kinetic zipper' model, *Biochemistry 36*, 9200.
13. Lednev, I. K., Karnoup, A. S., Sparrow, M. C., and Asher, S. A. (2001) Transient UV Raman Spectroscopy finds no crossing barrier between the peptide α-helix and fully random coil conformation, *J. Am. Chem. Soc. 123*, 2388.
14. Garcia, A. E., and Sanbonmatsu, K. Y. (2002) α-helical stabilization by side chain shielding of backbone hydrogen bonds, *Proc. Natl. Acad. Sci. U.S.A. 99*, 2782.
15. Zhang, W., Lei, H., Chowdhury, S., and Duan, Y. (2004) Fs-21 peptides can form both single helix and helix-turn-helix, *J. Phys. Chem. B 108*, 7479.

16. Sorin, E. J., and Pande, V. S. (2005) Exploring the helix-coil transition via all-atom equilibrium ensemble simulations, *Biophys. J 88*, 2472.
17. Chodera, J. D., Singhal, N., Pande, V. S., Dill, K. A., and Swope, W. C. (2007) Automatic discovery of metastable states for the construction of Markov models of macromolecular conformational dynamics, *J. Chem. Phys*. *126*, 155101.
18. Cornell, W. D. et al. (1995) A second generation force field for the simulation of proteins, nucleic acids, and organic molecules, *J. Am. Chem. Soc. 117*, 5179.
19. Duan, Y. et al. (2003) A point-charge force field for molecular mechanics simulations of protein based on condensed-phase quantum mechanical calculations, *J. Comput. Chem 24*, 1999.
20. Nymeyer, H., and Garcia, A. E. (2003) Simulation of the folding equilibrium of α-helical peptides: A comparison of the generalized Born approximation with explicit solvent, *Proc. Natl. Acad. Sci. U.S.A. 100*, 13934.
21. Hornak, V. et al. (2006) Comparison of multiple amber force fields and development of improved protein backbone parameters, *Protein: Struct. Funct. Bioinf. 65*, 712.
22. Jorgensen, W. L., Chandrasekhar, J., Madura, J. D., Impey, R. W., and Klein, M. L. (1983) Comparison of simple potential functions for simulating liquid water, *J. Chem. Phys*. *79*, 926.
23. Case, D. A. et al. (2005) The Amber biomolecular simulation programs, *J. Comput. Chem. 26*, 1668.
24. Garcia, A. E. (2004) Characterization of non-alpha helical conformations in ala peptides, *Polymer 45*, 669.
25. Young, W. S., and Brooks, C. L., III (1996) A microscopic view of helix propagation: N- and C-terminal helix growth in alanine helices, *J. Mol. Biol. 259*, 560−572.
26. Tobias, D. J., and Brooks, III, C. L. (1991) Thermodynamics and mechanism of α-helix initiation in alanine and valine peptides, *Biochemistry 30*, 6059−6070.
27. Lednev, I. K., Karnoup, M. C., Sparrow, M. C., and Asher, S. A. (1999) Alpha-Helix Peptide Folding and Unfolding Activation Barriers: A Nanosecond UV Resonance Raman Study, *J. Am. Chem. Soc. 121*, 8074−8086.
28. Mikhonin, A., Asher, S. A., Bykov, S., and Murza, A. (2007) UV Raman Spatially Resolved Melting Dynamics of Isotopically Labeled Polyalanyl Peptide: Slow α-Helix Melting Follows 310-Helices and π-Bulges Premelting, *J. Phys. Chem. B*. *111*, 3280−3292.

BI702112V